Microvoids in aramid-type fibrous polymers

M.G. Dobb, D.J. Johnson, A. Majeed and B.P. Saville
Textile Physics Laboratory, University of Leeds, Leeds LS2 9JT, UK

The presence of microvoids in aramid fibres has been suspected for some time. This communication reports their detection together with an investigation of their distribution and size in Kevlar 29 and 49 by electron microscopy and X-ray diffraction techniques. The voids appear to be located mainly around the periphery of the fibres and their dimensions measured from direct microscope examinations are compared with those obtained from a Guinier-type analysis of the low-angle X-ray diffraction data.

INTRODUCTION

Aramid fibres, such as the Kevlar group based on poly (*p*-phenylene terephthalamide) are finding increasing use in the fields of structural composites for aerospace and other reinforcement applications where high performance-weight ratios are advantageous.

The complex molecular structure of these fibres has been reported previously[1,2] and shown to consist of a unique system of radially oriented but axially pleated sheets, each sheet composed of an array of extended molecular chains stabilized laterally by hydrogen bonds.

It is found that the commercial versions of the fibre are generally characterized by intense but diffuse low-angle scattering on the equator of the X-ray diffraction patterns[3] similar to that exhibited by carbon fibres. This phenomenon arises from electron density discontinuities which may be due to either the presence of microvoids or regions of markedly different molecular packing in the fibres. Such features would be expected to be more accessible to water or other simple molecules whose inclusion might significantly alter the mechanical properties of the original fibre. Moreover, the mere presence of such structural discontinuities may have an adverse effect on the potential mechanical performance.

Unlike the voids in the carbon fibres[4,5] the characteristics of such features in Kevlar have not so far been studied in detail. Attempts have been made to define these regions by deposition of silver sulphide which should facilitate detection in the electron microscope and also enhance the scattering intensity for subsequent X-ray analysis. It should be noted that a similar technique has been employed for revealing the radial orientation in these fibres.[6] The purpose of this paper, therefore, is (a) to report and compare the size and distribution of voids in Kevlar 29 and 49 fibres and (b) to compare the results obtained from direct electron microscope examination with those from a Guinier analysis of the low-angle X-ray data.

EXPERIMENTAL

It will be convenient to consider this section under the following headings.

Specimen preparation

Two types of fibre were examined – Kevlar 29 and 49. Low-angle X-ray diffraction patterns were recorded from dry, wet and metal-stained specimens. Transmission electron micrographs were taken of the stained samples.

Fibres were impregnated with silver sulphide according to a two-stage process. The specimens were first treated with gaseous hydrogen sulphide at a pressure of 2×10^6 Pa at 20°C for 70 h. Subsequently the fibres were immersed in a 0.1 N aqueous solution of silver nitrate at 20°C for 24 h.

X-ray examination

Low-angle X-ray diffraction patterns of the fibres were recorded on film in a Searle-type camera (specimen – film distance 95 mm) mounted on a Hilger and Watt Y25 microfocus generator operating at 40 kV with a beam current of 3.5 mA. The X-radiation was nickel-filtered CuKα. For most samples the exposure time on Kodirex film was 24 h, except in the case of metal-stained specimens when it was only 2 h. The camera chamber was evacuated to a pressure of 26 Pa using phosphorous pentoxide as a desiccant. Wet samples were sealed in a glass capillary tube prior to examination.

Microdensitometry

Equatorial scans through the low-angle regions of the recorded diffraction patterns were made using a Joyce-Loebl microdensitometer equipped with a digital output facility. It was ensured that the total scattered intensity at a particular S value was determined using a sufficiently long slit. Guinier plots of log (intensity) vs. S^2 were constructed from the data, where $S = 2 \sin\theta/\lambda$; where θ is the Bragg angle and λ the wavelength of the radiation.

The axial width of the low-angle scatter was estimated from other intensity scans taken parallel to the meridian at known values of S. The widths at half height (h) of each scattering profile were determined at known values of S and the angular width (β) calculated from the expression $\tan(\beta/2) = h/2S$.

Electron microscope examination

Treated fibres were embedded in Spurr resin and longitudinal and oblique (45° to the fibre axis) sections were cut on an ultramicrotome using a diamond knife. It should be noted that oblique sections which can subsequently be tilted through 45° in the microscope were preferred to transverse sections owing to the massive disruption of the latter experienced during microtomy.

0032-3861/79/101284-05$02.00

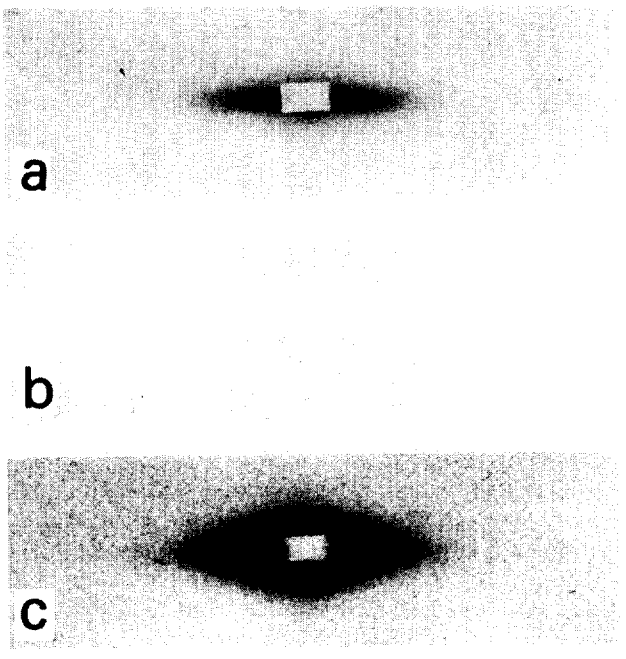

Figure 1 Low-angle X-ray patterns of Kevlar 49 fibres: (a) dry; (b) wet and (c) stained with silver sulphide

All specimens were examined in a JEOL 100CX transmission microscope equipped with a side-entry gonimeter and operating at 100 kV. The magnification of the microscope was calibrated using the 1.19 nm lattice fringes from the 201 planes in platinum phthalocyanine crystals. Micrographs of the same crystals were also recorded at lower magnification settings. By comparing the dimensions of common features, the magnifications of given instrumental settings were calibrated.

RESULTS

X-ray data

Figures 1a and *1b* show the low-angle X-ray scattering of dry and wet specimens, respectively, of Kevlar 49. It is clear that the presence of moisture markedly reduces the intensity of the equatorial scatter. Moreover, the change in intensity can be reversed by pumping dry the wet sample. These effects can be explained in terms of the uptake of water reducing inherent electron density differences within the fibre.

Since regions in the polymer are accessible to water molecules it seemed logical to expect that other simple molecules might also be able to penetrate these regions. *Figure 1c* depicts the low-angle pattern from a stained dry specimen where an intensification of the scattering is clearly evident in comparison with *Figures 1a* and *1b*. It would appear that localized deposition of the metal sulphide has occurred so increasing the electron density differences within the fibre.

In order to compare estimates of void dimensions by dissimilar methods (namely X-ray analysis of the low-angle scattering and direct electron microscope observations) the two evaluations were carried out independently.

Without information other than that provided by the distribution of scattered intensity it is necessary to make certain assumptions in any X-ray analysis. The marked elongation of the scattering along the equator suggests that the voids are asymmetric having a preferred orientation

Table 1 Void dimensions

Specimen		Void width (nm)	Void width (nm)	Void length (nm)
		X-ray data	*EM* data	
Kevlar 29	Dry untreated	7.6	–	–
	Dry stained	5.8	6.1 $\sigma = 1.1$	24.7 $\sigma = 7.8$
Kevlar 49	Dry untreated	10.6	–	–
	Dry stained	5.0	5.6 $\sigma = 0.8$	25.1 $\sigma = 8.0$

σ is the standard deviation.

with their long axes approximately parallel to the fibre axis. Moreover, the monotonic nature of the plots of the normalized log (Intensity) vs. S^2 for unstained and stained specimens of Kevlar 29 and Kevlar 49 shown in *Figures 2* and *3*, respectively, indicate the apparent absence of a preferred separation of the voids.

Using only the above considerations it would seem reasonable to apply a simple Guinier approximation[7] to determine the void widths. The relation between the intensity of scattering (I) and values of S for a monodisperse system of particles with definite orientation, assuming each is an ellipsoid of dimensions a, a and va is:

$$\log_{10} I(S) = \frac{-4\pi^2 S^2}{5} (a)^2 \log_{10} e + \text{constant}$$

Hence the slopes of the extrapolated curves at $S = 0$ are directly related to the particle radius (a) by the expression

$$a = 0.539\,(\text{Slope})^{1/2}$$

Table 1 shows the calculated values of the void diameters for the different specimens.

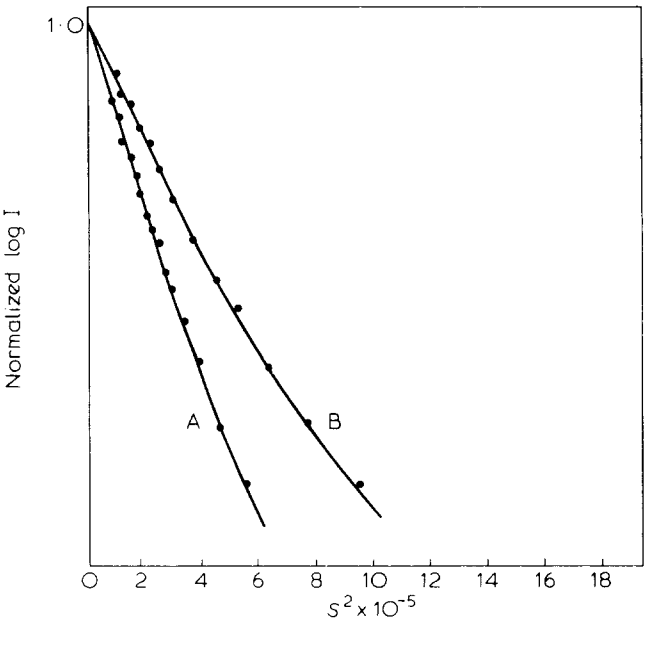

Figure 2 Guinier plot of normalized log I vs. S^2 for Kevlar 29: A, stained; B, unstained

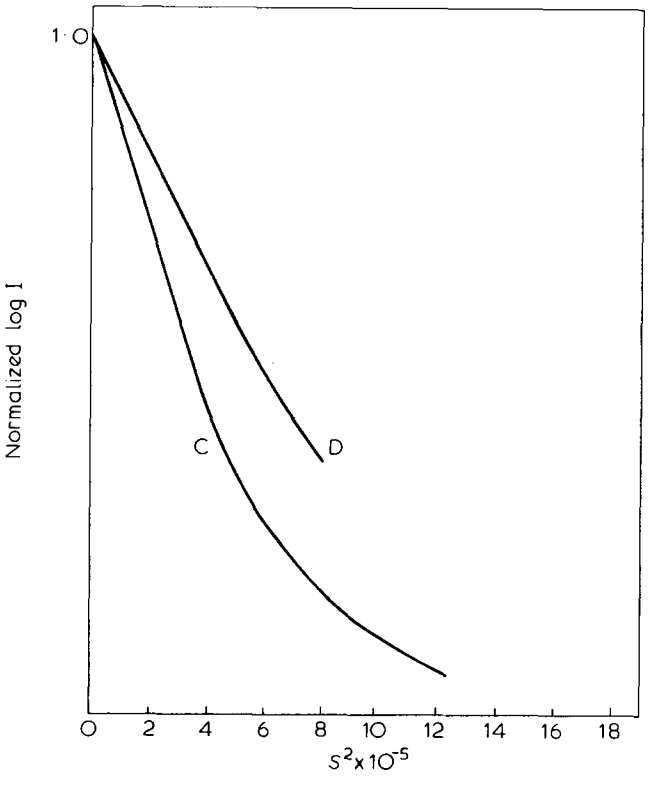

Figure 3 Guinier plot of normalized log *I* vs. S^2 for Kevlar 49: C, unstained; D, stained

For a system of voids generally elongated along the fibre axis, the angular width (β) of the equatorial scatter will be a function of both void length and misorientation. However, the component due to the void length will approach zero at high values of S (i.e. β should approach a constant value due to misorientation).[8] The constant values of β which may be regarded as a measure of misorientation of the voids relative to the fibre axis are shown in *Table 2*. No reliable estimates of the void length were made owing to instrumental limitation.

Electron microscope data

The micrographs, *Figures 4a* and *4b* and *5a* and *5b*, show transverse and longitudinal aspects of stained specimens of Kevlar 29 and Kevlar 49. The most distinctive feature is the highly localized peripheral deposition of silver sulphide in both fibres. There is also evidence showing a tendency for the metal to be located along radii of the fibres away from the high concentration of sub-surface deposits. In the case of Kevlar 29 the concentration of scattering centres is much higher than in Kevlar 49. The silver sulphide in both specimens appears to be deposited in the form of aggregates having an approximately circular cross-section whose dimensions are given in *Table 1*. Measurements of the average length of the aggregates are also shown and were obtained from examination of longitudinal sections. In both types of fibre there is a strong tendency for the aggregates to be oriented parallel to the fibre axis.

It is also interesting to note that much larger aggregates of metal approximately 0.08 μm across and of length up to 16 μm are frequently encountered particularly near the centre of Kevlar 49 fibres which at present have been tentatively identified with the presence of large scale cracks.

Table 2 Void and crystallite orientation

Specimen		Angle β (degrees)	Crystallite orientation (200) degrees
Kevlar 29	Dry untreated	18.7	11.0
	Dry stained	22.9	–
Kevlar 49	Dry untreated	15.4	9.0
	Dry stained	18.3	–

DISCUSSION

It would seem reasonable to associate the reduction in intensity of the low-angle equatorial scatter after moisture uptake with the initial presence of low density components in the fibres which we interpret in terms of a system of microvoids. The electron microscope evidence of stained specimens strongly supports this concept and moreover indicates that the microvoids are rod-shaped with their long axes almost parallel to the fibre axis. In micrographs, *Figures 5a* and *5b*, the stained regions, identified with the microvoids, often appear to be isolated from each other. However, this feature is difficult to reconcile with the proven accessibility towards reagent molecules. Thus it would be logical to assume that during treatment the microvoids are connected by a fine capillary network to the fibre surface. The fine dimensions of the envisaged capillary system are probably altered by subsequent dehydration of the specimen so that their presence in micrographs is not apparent.

Table 1 shows reasonable agreement in the lateral sizes of the stained microvoids estimated using two different techniques namely X-ray diffraction and bright field transmission electron microscopy. The microscope data was obtained by direct measurement on micrographs whereas the X-ray method is dependent on the assumptions discussed below.

Microvoid concentration

The X-ray analysis assumes that the distribution of microvoids has no effect on the scattering profile. However, close-packing of the voids is evident in the electron micrographs (see *Figure 4*), particularly in the peripheral regions of the fibres. Consequently, the slopes of the Guinier plots at $S = 0$ probably include contributions from interference effects between scattering sites. According to Guinier[7] the measured radius would be lower than the true value.

Size distribution

For purposes of analysis it has been assumed that the microvoids are regular in size. However, if the scattering sites exhibit a distribution in size then since the slope of the Guinier plot is proportional to the square of the radius it would be expected that the contribution of the larger microvoids towards the X-ray scattering profile would be greater, thus tending to produce a higher value for the radius than the arithmetic mean.

Presence of cracks

The presence of internal cracks, occasionally seen in stained specimens, whose dimensions are relatively larger

Figure 4 Micrographs of transverse sections through stained Kevlar 29 (a) and Kevlar 49 (b), respectively. Scale markers 1.0 μm and 0.5 μm

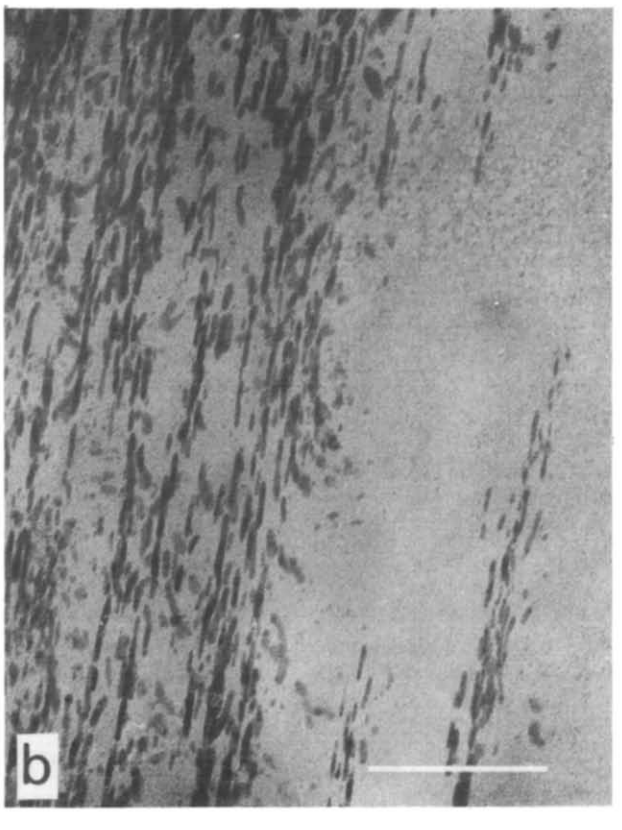

Figure 5 Micrographs of longitudinal sections through stained Kevlar 49 (a) and Kevlar 29 (b), respectively. Scale markers 0.2 μm

than those of the microvoids will tend to give enhanced scattering at low S values. Since the radius is directly related to the slope of the Guinier plot in this region, then a higher average value for the microvoid size will be obtained.

Shape of microvoids

In the X-ray analysis it has been assumed that the microvoids are circular in cross-section. Clearly, any departure from this assumption will lead to erroneous results for the dimensions. However, examination of electron

micrographs indicates that such an assumption is reasonable.

From the results shown in *Table 1*, there is a marked discrepancy between the void widths of unstained and stained specimens. In both unstained Kevlar 29 and Kevlar 49, the calculated widths are much greater than those estimated for the stained specimens.

It may be argued that the deposition of metal sulphide does not reflect the original size and distribution of the voids within the fibres due to either structural changes brought about by the staining process or the mode of aggregation of the stain. Alternatively, it would appear that only a proportion of the voids are accessible to the stain. Indeed the system of voids may have two components, one where the voids are completely isolated and another where the voids are connected directly to the fibre surface.

At present it is not possible to distinguish between these possibilities; however, the results do emphasize the need for extreme caution in interpreting data from 'labelled' specimens.

Measurements on micrographs of the metal deposits in stained specimens indicate that the length to width ratio is approximately four. The microvoids in Kevlar 29 have almost the same length as those detected in Kevlar 49 having values of 24.7 nm (σ = 7.8 nm) and 25.1 nm (σ = 8.0 nm), respectively.

Values for the orientation angle of the microvoids shown in *Table 2* are higher than those obtained for the orientation of the crystallites estimated from the angular spread of the (200) reflection. This discrepancy in angle may arise from the dissimilar size distribution profiles of the voids and the crystallites so that the estimates of angular width at half height reflect different percentages of the scattering population in each case. Thus the two orientation angles would not be directly comparable. Nevertheless, there is a general tendency for the majority of voids to be aligned approximately parallel to the *C*-axis of the crystallites. Moreover, the observed values indicate that the staining process appears to have a small effect on the orientation of the voids.

It would seem logical at this stage to consider the origin of the system of voids characterized during this work, particularly since their presence may be associated with a loss in potential mechanical performance of the aramid fibres. As considerable reduction in volume occurs during removal of the solvent to form well-ordered fibres, some voiding would be expected to arise during the solidification of the polymer in the coagulating bath of the extrusion process.[9]

Thus regions corresponding to the inclusion of coagulating medium or residual solvent may be permanently incorporated within the fibre structure. The distribution of voids would then reflect differences in rates of solidification between different parts of the fibre. Subsequent heat treatment may also produce further void-formation particularly since some localized shrinkage would be expected from the improvement in molecular packing associated with the observed increase in crystallite size.[9]

As implied previously, the presence of voids will affect the mechanical properties of the fibres. Voids will tend to reduce both the potential lateral and tensile strengths of a fibre. Moreover, if the voids have a length to width ratio greater than unity then the effect will be greater on the lateral than on the tensile properties thus contributing to a low compressional strength. Since such features are located predominantly around the periphery of the fibres then one would expect the low compressional strength to have most effect on the bending characteristics.

In addition to the relatively small effect of the voids on the tensile properties arising from the effective reduction in cross-sectional area, a more marked contribution will arise from the observed long (up to 16 μm) macrocracks lying at small angles to the fibre axis. Fracture would be facilitated by propagation of these cracks over extensive lengths to the weak outer layers of the fibre.

ACKNOWLEDGEMENTS

The authors would like to thank the Science Research Council for financial support during this work. We are also indebted to Drs M. Sotton and R. Hagge of L'Institut Textile de France, Paris, for carrying out the staining treatment.

REFERENCES

1 Dobb, M.G., Johnson, D.J. and Saville, B.P. *J Polym Sci (Polym Symp)* 1977, **58**, 237
2 Dobb, M.G., Johnson, D.J. and Saville, B.P. *J Polym Sci (Polym Phys Ed)* 1977, **15**, 2201
3 Northolt, M.G. and Van Aartsen, J.J. *J Polym Sci (Polym Symp)* 1977, **58**, 283
4 Johnson, D.J. *First Int Conf Carbon Fibres, Plastics Institute* 1971, p 52
5 Fourdeux, A., Perret, R. and Ruland, W. *First Int Conf Carbon Fibres,* Plastics Institute 1971, p 57
6 Hagege, R., Jarrin, M. and Sotton, M.J. *J Microscopy* 1979, **115**, 65
7 Guinier, A. and Fournet, G. 'Small Angle Scattering of X-rays', Wiley, New York, 1955
8 Ruland, W. *J Polym Sci* 1969, **28**, 143
9 Blades, H. US Pat. 3 869 430; Br. Pat. 391 501. (Assigned to E.I. du Pont de Nemours & Co.)
10 Majeed, A. *PhD Thesis* University of Leeds (1979)